Journal of Ethnopharmacology 353 (2025) 120335

Contents lists available at ScienceDirect

Journal of Ethnopharmacology

journal homepage: www.elsevier.com/locate/jethpharm

Achyrocline satureioides: *in silico* and *in vivo* evaluation of the potential neuroprotective effect of the aqueous extract

Peterson Alves Santos [a,b], Pricila Pflüger [b,c], Marilise Brittes Rott [d], Hipólito Gómez-Couso [e], Ionara Rodrigues [d], Patricia Pereira [a,b], José Ángel Fontenla [b,*]

[a] *Laboratory of Neuropharmacology and Preclinical Toxicology, Institute of Basic Health Sciences, Federal University of Rio Grande do Sul, Porto Alegre, 90050-170, Brazil*
[b] *GI-1684 Laboratory of Central Nervous System Pharmacology (Faculty of Pharmacy), Department of Pharmacology, Pharmacy and Pharmaceutical Technology, University of Santiago de Compostela, Santiago de Compostela, 15782, Spain*
[c] *Center for Research in Molecular Medicine and Chronic Diseases (CIMUS). University of Santiago de Compostela, Santiago de Compostela, 15782, Spain*
[d] *Institute of Basic Health Sciences (ICBS), Federal University of Rio Grande do Sul, Porto Alegre, 90050-170, Brazil*
[e] *Laboratory of Parasitology, Department of Microbiology and Parasitology, Faculty of Pharmacy/Institute of Food Research and Analysis, University of Santiago de Compostela, Santiago de Compostela, 15782, Spain*

A R T I C L E I N F O

JEL classification:
Central Nervous System

Keywords:
Traditional medicine
Neurodegenerative diseases, *in silico*
Caenorhabditis elegans
Achyrocline satureioides

A B S T R A C T

Ethnopharmacological relevance: Achyrocline satureioides (Lam.) DC is traditionally used as an infusion in several South American countries to treat various health conditions, including those affecting the central nervous system. Recent studies indicate its potential neuroprotective effects and suggest possible benefits in alleviating neurological symptoms in COVID-19 patients. However, its direct impact on the central nervous system remains underexplored.

Aim of the study: This study aimed to assess the *Achyrocline satureioides* effects infusion on dopaminergic and cholinergic neurodegeneration patterns induced by reserpine or manganese in *Caenorhabditis elegans* (*C. elegans*), and to perform *in silico* analysis of the primary bioactive compounds in the *Achyrocline satureioides* aqueous extract (ASAE).

Materials and methods: Using *C. elegans* as an experimental model, we evaluated the neuroprotective effects of the aqueous extract of *Achyrocline satureioides* on dopaminergic and/or cholinergic neurodegeneration induced by reserpine or manganese. Behavioral assays evaluated the preservation of motor function and pharyngeal pumping in nematodes. In addition, *in silico* studies were performed with the bioactive compounds identified in the extract and compared with drugs currently used for Parkinson's and Alzheimer's diseases.

Results: In the studies with *C. elegans*, neurodegeneration induced by reserpine (60 μM) was attenuated at the highest extract concentration (25 mg/ml) tested. Additionally, animals previously exposed to the extract exhibited improved behavior at both concentrations (10 and 25 mg/ml). When neurodegeneration was induced by manganese (50 mM), both concentrations of the ASAE reduced neurodegeneration and improved behavior. *In silico* studies evaluated the absorption, distribution, metabolism, and elimination (ADME) properties and molecular docking of identified compounds against established targets associated with neurodegenerative diseases.

Conclusions: The *Achyrocline satureioides* bioactive compounds appear to influence pathways targeted by current therapies for Parkinson's and Alzheimer's diseases. The aqueous extract demonstrated promising neuroprotective potential and modulation of the dopaminergic and cholinergic systems, reducing neurodegenerative damage and enhancing behavior.

* Corresponding author. Department of Pharmacology, Pharmacy and Pharmaceutical Technology, Faculty of Pharmacy. University of Santiago de Compostela, 15782, Santiago de Compostela, Spain.
E-mail addresses: peterson.alves@ufrgs.br (P.A. Santos), pricila.fernandes.pfluger@usc.es (P. Pflüger), marilise.rott@ufrgs.br (M.B. Rott), hipolito.gomez@usc.es (H. Gómez-Couso), ionara@ufrgs.br (I. Rodrigues), patriciapereira@ufrgs.br (P. Pereira), joseangel.fontenla@usc.es (J.Á. Fontenla).

https://doi.org/10.1016/j.jep.2025.120335
Received 10 April 2025; Received in revised form 15 July 2025; Accepted 27 July 2025
Available online 31 July 2025

1. Introduction

With the aging population, age-related diseases have become an increasing concern, especially those affecting the central nervous system (CNS). Among these, neurodegenerative diseases pose a significant challenge to healthcare systems due to their complexity, complicating both diagnosis and treatment. Recent epidemiological data suggest that Parkinson's disease (PD) is becoming more prevalent, with estimates indicating that it affects approximately ten million people worldwide. Furthermore, PD is considered the second most prevalent neurodegenerative disease after Alzheimer's disease (AD) (Driver et al., 2009). The clinical manifestations of PD are closely associated with the degeneration of nigrostriatal dopaminergic neurons. A decrease in dopamine levels leads to progressive motor deficits, while neurotransmitter imbalances contribute to excitotoxicity mechanisms, intensifying motor symptoms. Additionally, alpha-synuclein aggregation, oxidative stress, and neuroinflammation result in neuronal death, contributing to cognitive and psychiatric complications (Park et al., 2007; Brochard et al., 2008; Krawczuk et al., 2024).

The infusion of *Achyrocline satureioides* (*A. satureioides*) inflorescences, commonly known as "marcela," has been widely used in South America as an aqueous extract for neuroprotective purposes. Belonging to the family Asteraceae, *A. satureioides* has traditionally been used to alleviate nervous symptoms associated with neurological disorders (Gross et al., 2019; Megret et al., 2013), as well as anti-inflammatory potential (Moresco et al., 2017). *A. satureioides* was included in the Brazilian Pharmacopoeia in 2001, highlighting its longstanding popularity (Retta et al., 2012).

Experimental evidence suggests that *A. satureioides* can promote neurodifferentiation, reduce brain damage, and enhance neuronal cell viability (Martínez-Busi et al., 2019). Recently, a study demonstrated that the use of this species was associated with improved neurological symptoms in COVID-19 patients (Bastos et al., 2023). Its bioactive compounds, including quercetin (Q) and luteolin (L), are well-known for their antioxidant properties, potentially offering protection against oxidative stress-induced neuronal damage.

Given these considerations, multi-target strategies offering neuroprotection are increasingly necessary in therapeutic approaches. Interest in phytochemicals and herbal medicines is growing, with a focus on isolated bioactive compounds. However, in the context of limited resources and restricted access to pharmaceuticals in underdeveloped regions, ethnopharmacological strategies present an accessible alternative. Recent studies indicate that plants rich in flavonoids, such as Q and L, hold promising potential for treating neurological disorders, including PD and AD (Costa et al., 2016; Kim et al., 2020; Zhang et al., 2020).

The main objective of this study was to evaluate bioactive compounds from *A. satureioides* in *in silico* studies and ASAE in two models of neurodegeneration in *C. elegans*.

2. Material and methods

2.1. Inflorescences and Achyrocline satureioides aqueous extract (ASAE)

The inflorescences were supplied by the company Kampo de Ervas (CNPJ: 08.898.383/0001–79). Access to genetic heritage in Brazil was registered in the SisGen system (A928BF2). According to the Brazilian Pharmacopoeia (ANVISA, 2024) (http://bibliotecadigital.anvisa.gov.br/jspui/handle/anvisa/12413), the aqueous extract was prepared from the inflorescences of *A. satureioides* by extraction via infusion in hot water at 80 °C for 15 min, with a solvent ratio of 1:10 (inflorescences in g/ml of water), yielding a stock solution of 100 mg/ml. For treatments, this stock solution was diluted to concentrations of 10 mg/ml and 25 mg/ml. The plant name was verified with the World Flora Online database (http://www.worldfloraonline.org) on March 28, 2024 (Bastos et al., 2023).

The quality and composition of the compounds evaluated in this study were previously described by Bastos et al. (2023), and the main compound contents were measured using high-performance liquid chromatography, as outlined by Barioni et al. (2013) and Moresco et al. (2017).

2.2. Chemicals

Reserpine (RES), manganese, and other reagents were sourced from Sigma-Aldrich (Merck Life Science S.L.U., Madrid, Spain).

2.3. Caenorhabditis elegans (C. elegans)- strain and maintenance

The strains used in this study included Wild-type Bristol (N2), BY200 (*dat-1*[*vtIs1*{*Pdat-1::GFP*, *pRF4*(*rol-6*(*su1006*))}]), and LX929 (*vsIs48* [*unc-17::GFP*]). They were grown on Nematode Growth Medium (NGM) agar plates seeded with a lawn of deactivated *Escherichia coli* strain OP50 as feed, maintained under standard conditions. For experiments, the animals were synchronized using a bleaching solution (2.5 % hypochlorite, 1M NaOH, and distilled water). A 30 % sucrose gradient was applied to isolate the remaining eggs, which were then washed, centrifuged, and resuspended in complete Medium K. Cultures were shaken at 20 °C, and after 12 h, synchronized L1 worms were used for assay (Sammi et al., 2022; Khanna et al., 1997).

The in vivo studies were authorized by process 40462 from the Research Commission of the Federal University of Rio Grande do Sul (COMPESQ/UFRGS). As this study involves an invertebrate animal model, it does not require approval from an animal ethics committee, per applicable legislation.

2.4. Pharmacological treatments

Upon reaching the L1 stage (12 h), the populations were washed from the NGM plates and treated with an aqueous extract of *A. satureioides* in liquid medium for 24 h. Based on our previous published studies on the safety and toxic effect of ASAE in *C. elegans* we chose to use concentrations of 10 and 25 mg/ml (Santos et al., 2024). Control groups, which received no treatment, were subjected to the same conditions. At the end of the treatment period (L3 stage), the animals were exposed to either manganese or RES. For manganese exposure, populations from both the treated and control groups were divided into samples of approximately 1500 animals and exposed to 50 mM manganese (BY200 and N2) or 100 mM manganese (LX929 and N2) in 85 mM NaCl for 30 min under gentle and continuous agitation. After exposure, the samples were washed three times and then kept for 24 h before evaluations (Schetinger et al., 2019; Au et al., 2009).

For RES exposure (48 h), adaptations of the experimental procedures by Guedes and collaborators (Guedes et al., 2023) were implemented. The samples were separated as previously described and exposed to 60 μM of RES (all strains). Negative controls (NC or untreated worms) and vehicle controls (acetic acid-AA-0.012 %) were also conducted. Subsequently, the samples were washed three times and evaluated.

2.5. Dopaminergic neurodegeneration

The BY200 strain, which was previously treated with ASAE (10 and 25 mg/ml) and exposed to RES (60 μM) or manganese (50 mM), was evaluated after exposure to the neurotoxic agent. The animals were placed on histological slides and immobilized with sodium azide (0.5 M). Photographs of the cephalic region of the worms were taken at 60× magnification using a microscope to evaluate the CEP neurons and dopaminergic dendrites. Twenty worms per treatment were analyzed, and the experiments were conducted in duplicate. Images were analyzed using NIH ImageJ software (Reckziegel et al., 2015; Gavet and Pines, 2010).

2.6. Cholinergic neurodegeneration

The LX929 strain, was pre-treated with ASAE (10 and 25 mg/ml) or left untreated, and after it was exposed to RES (60 μM) or manganese (100 mM). The animals were placed on histological slides and immobilized with sodium azide (0.5 M). Photographs of the entire animal were taken at 40× magnification under a microscope, aiming to evaluate all cholinergic neurons extending from the cephalic region along the ventral muscle groups to the caudal region. Twenty worms per treatment were analyzed, and the experiments were conducted in duplicate. Images were analyzed using NIH ImageJ software (Schetinger et al., 2019).

2.7. Body bend/basal slowing (behavior modulated by dopamine)

The animals were washed following the ASAE (10 and 25 mg/ml) treatment and exposures to RES (60 μM) or manganese (100 mM). Body bends were assessed by placing approximately 20 worms on plates seeded with a circular lawn of OP50 or on unseeded plates. After 5 min, the number of body flexions was counted to evaluate the locomotor rate on both seeded and unseeded plates over a 20 s period (Sawin et al., 2000).

The basal deceleration index was determined as described by Cooper and Raamsdonk (2018) to assess the rate of recovery of the basal response. Following injury, animals with dopaminergic damage were maintained for 24 h on plates containing ASAE (10 and 25 mg/ml), without prior treatment.

2.8. Pharyngeal pumping (behavior modulated by acetylcholine)

Pharyngeal pumping was assessed as previously described Schetinger et al. (2019). After the ASAE (10 and 25 mg/ml) treatment and the exposure to the neurotoxic agent RES (60 μM) or manganese (100 mM), strain N2 animals were washed and placed on solid NGM medium. The number of contractions, indicated by the opening and closing of the pharyngeal bulb, was counted for 10 s under a microscope at 10 × magnification by two independent evaluators. Twenty worms per treatment were analyzed, and the experiments were performed in duplicate (Schetinger et al., 2019).

2.9. Designing molecules

To understand the properties of 3-O-methylquercetin (3OMQ), achyrobichalcone (ACB), quercetin (Q), luteolin (L), and the reference drugs used in PD and AD, the 2D structures of the compounds were obtained using ChemDraw software (version Ultra 21.0, PerkinElmer Informatics, Waltham, MA, USA), the Marvin JS program (https://marvinjs-demo.chemaxon.com/latest/demo.html), and KingDraw (http://www.kingdraw.cn/en/). These structures were then converted into a single database file in either SMILES or SDF format and transformed into 3D structures using the Open Babel 2.3.2 online tool (https://www.cheminfo.org/Chemistry/Cheminformatics/FormatConverter/index.html).

2.10. Prediction of physicochemical and ADME properties

The physicochemical and pharmacokinetic properties of the 3OMQ, ACB, Q, and L were determined using several online resources, including the Molinspiration program (Molinspiration Cheminformatics Software, https://www.molinspiration.com/), SwissADME (http://www.swissadme.ch/), and pkCSM (https://biosig.lab.uq.edu.au/pkcsm/prediction). The results obtained were compared with those of reference drugs for PD (L-DOPA and apomorphine) and AD (galantamine and donepezil). The metabolism and ACB metabolites were evaluated using BioTransformer 3.0 (https://biotransformer.ca/).

2.11. Prediction of ability to cross the blood-brain barrier (BBB)

The prediction of permeability through the blood-brain barrier (BBB) was evaluated using the Online BBB Predictor (https://www.cbligand.org/BBB/predictor.php). This assessment employed two algorithms, support vector machine (SVM) and AdaBoost, alongside four types of fingerprints: MACCS, Openbabel (FP2), Molprint 2D, and PubChem.

2.12. Prediction of the transport mechanism at the BBB via LAT1

The compounds ACB, 3OMQ, Q, and L, share structural similarities with L-dopa, gabapentin, and natural essential amino acids (tyrosine and phenylalanine), all of which utilize the large neutral amino acid transporter (LAT1) to cross the BBB. Docking analyses using the CB-Dock2 program were conducted (described in section 2.15) to evaluate their binding affinity to LAT1 and to compare their potential for passage through the BBB into the CNS with that amino acids and drugs previously identified as substrates for this transporter. The structure of the LAT1 receptor was obtained from the Protein Data Bank (PDB, https://www.rcsb.org/) under entry 6IRS, with a resolution of 3.30 Å.

2.13. Determining targets

To identify the macromolecular targets for potential interactions with the compounds of interest, we utilized SwissTargetPrediction (https://www.expasy.org/resources/swisstargetprediction).

2.14. Toxicity evaluation

The potential oral toxicity of the compounds was assessed by predicting their lethal dose (LD50) classes using the ProTox-II online database (https://tox-new.charite.de/protox_II).

Additionally, potential cardiotoxicity, the maximum recommended tolerated dose (MRTD), and mutagenic activity were evaluated using the Ames test through the pkCSM program, which estimates the toxic dose threshold for humans.

2.15. Docking studies

The proteins with the highest binding affinity were evaluated using the CB-Dock2 program (https://cadd.labshare.cn/cb-dock2/index.php), a protein-ligand blind docking tool. The structures of the proteins were obtained from the PDB protein database (RCSB PDB). The ligands 3OMQ, ACB, Q, and L, along with the synthetic reference control, were designed using the Marvin JS program and converted into 3D structures in Avogadro software (Avogadro) using the Open Babel 2.3.2 tool.

2.16. Graphical representation and statistical analyses

The graphical representation and statistical analysis were performed using GraphPad Prism software (Version 8.0.1; GraphPad Software, Boston, MA, USA). Differences observed in the nematodes exposed to test solutions and the control were analyzed using One-way ANOVA, followed by Dunnett's test. Results are expressed as the mean ± standard error of the mean (SEM) from at least three samples (N = 3). Differences were considered significant at $p \leq 0.05$.

Figures, illustrations, and schematic representations were created using bioRender software (https://www.biorender.com/).

3. Results

3.1. Achyrocline satureioides aqueous extract (ASAE)

Based on the previously described extraction method for Bastos et al. (2023), which resembles the traditional preparation and consumption of infusions, the concentrations of ASAE used in these studies were 10

mg/ml and 25 mg/ml (w/v). The quantities of *A. satureioides* inflorescences and the corresponding infusion volumes were calculated, with Table 1 presenting the values of the compounds of interest at these concentrations.

The chromatographic representation of the ASAE (1 %) showing the main flavonoids found in the traditional formulation is shown in Fig. 1.

Additional information on UHPLC analysis can be found in the references Bastos et al. (2023 and 2025), and Santos et al. (2024).

3.2. In vivo studies

In this study, *C. elegans* was employed as an alternative model to investigate new compounds with potential neuroprotective activity. We mimicked the degradation of dopaminergic and cholinergic neurons by exposing the nematodes to two neurotoxins: RES and manganese. The ASAE treatments administered were 10 mg/ml and 25 mg/ml.

3.2.1. ASAE mitigates dopaminergic neurodegeneration induced by reserpine and manganese

Upon examining the neuronal bodies in the posterior cephalic sensilla (CEP) of BY200 nematodes (Fig. 2) exposed to RES (positive control for neurodegeneration, 2a) or manganese (positive control for neurodegeneration, 2c), a decrease in fluorescence was observed. ASAE demonstrated the ability to prevent this damage caused by both RES (2a/b) and manganese (2c/d). Notably, ASAE at 10 mg/ml did not exhibit protective capacity against RES (2a); only the 25 mg/ml concentration proved effective. Conversely, both ASAE concentrations effectively prevented damage induced by manganese (2b).

In the context of dopaminergic neurons, degradation of the posterior (head) neurons was observed in animals exposed to RES (3a) and manganese (3b) (Fig. 3). An assessment of the integrity of these branches revealed that ASAE provided protective effects comparable to those observed previously. Interestingly, while the previous figure indicated that RES (positive control for neurodegeneration, 2a) significantly impacted the neuronal body region more than manganese (positive control for neurodegeneration, 2c), the relationship was reversed in this instance. Manganese (positive control for neurodegeneration, 3b) caused more damage to the neurites than RES (positive control for neurodegeneration, 3a).

3.2.2. Neuroprotection against cholinergic disruption: ASAE attenuates morphological and functional deficits

For comparative purposes, despite the proportionally lower damage to the cholinergic system caused by the evaluated toxicants (RES and manganese) compared to the dopaminergic system, we found concentrations of these toxicants capable of altering the neuronal morphology of the cholinergic system in the *C. elegans* strain LX929 (Fig. 4).

The results with ASAE (10 and 25 mg/ml) were like those obtained with the dopaminergic system in the *C. elegans* BY200 strain. Against RES (4a), only ASAE at 25 mg/ml effectively minimized the toxin's impact on cholinergic neurons. In contrast, exposure to manganese (4b) at a higher and more non-selective concentration (100 mM) allowed ASAE at both 10 and 25 mg/ml to prevent neuronal damage.

3.2.3. ASAE restores behavioral and neuromuscular functions impaired by neurotoxins

CEP neurons, along with anterior deirid (ADE) and post-deirid (PDE) neurons, are responsible for the behavior known as basal deceleration, a locomotor response to the presence of a bacterial patch, mediated by dopamine. In other words, low levels of dopamine prevent the animal from exhibiting this search and deceleration behaviour in the presence or absence of food.

As illustrated in Fig. 5, for the positive controls for neurodegeneration (PC), the animals exposed to RES (60 μM) and manganese (50 mM) maintained similar body curvature values regardless of the presence of OP50 feed, indicating a clear dysfunction in feed sensing. However, treatment with ASAE prevented and restored the damage caused by RES or manganese, allowing the animals to exhibit normal discrimination behavior in both the presence and absence of food (OP50). This demonstrates the neuroprotective capacity of ASAE.

The potential to prevent the progression of dopaminergic damage is a crucial aspect of therapeutic strategies for PD. While improving motor deficits is the primary objective of treatments like L-dopa, it is essential to explore alternative interventions. To evaluate whether ASAE could modulate motor deficits and prevent or reverse dopaminergic impairment in *C. elegans* exposed to RES or manganese, we administered treatments immediately after the injury and maintained them for 24 h.

As illustrated in Fig. 6, dysfunction is markedly evident in the groups exposed to RES (6a) and manganese (6b) without ASAE (positive control groups for neurodegeneration). In contrast, both ASAE treatments (10 and 25 mg/ml) significantly improved the animals' basal deceleration response index, suggesting a reversal of dopaminergic damage.

In the pharyngeal pumping evaluation (Fig. 7), which is indicative of proper cholinergic transmission, *C. elegans* treated solely with RES (60 μM, 7a) or manganese (100 mM, 7b) exhibited a significant reduction in pumping capacity. However, treatment with ASAE (10 or 25 mg/ml) effectively restored normal pharyngeal pumping at both concentrations for both neurotoxins.

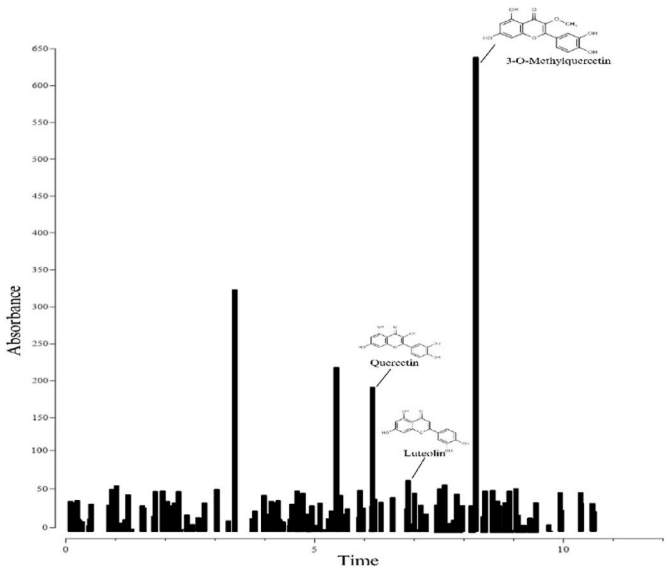

Fig. 1. Identification of the main flavonoid compounds by UHPLC of ASAE 1 % and with illustration of the compounds of interest and commercially available quercetin, luteolin, and 3-O-methylquercetin.

Table 1
Concentrations values of Q, L, 3OMQ and ACB in the ASAE 1 % (10 mg/ml) and 2.5 % (25 mg/ml). Data calculated from https://doi.org/10.1002/ptr.7976.

ASAE (mg/ml)	Inflorescences (% w/v)	Q (μg/ml)	L (μg/ml)	3OMQ (μg/ml)	ACB (μg/ml)
10	1 %	18.3	6.9	77.5	9.5
25	2.5 %	45.75	17.25	193.75	23.75

3.3. In silico studies

3.3.1. Physicochemical characterization of ASAE bioactive compounds

The physicochemical properties and ADME analysis were conducted using two different software packages: Molinspiration and SwissADME.

The same metabolites produced in the gut are also identified in other human biosystems as indicated by the software. The reaction remains consistent across these systems, facilitated by a class of enzymes known as hydrolases (EC 3.7.1), specifically ketone-specific hydrolases. These

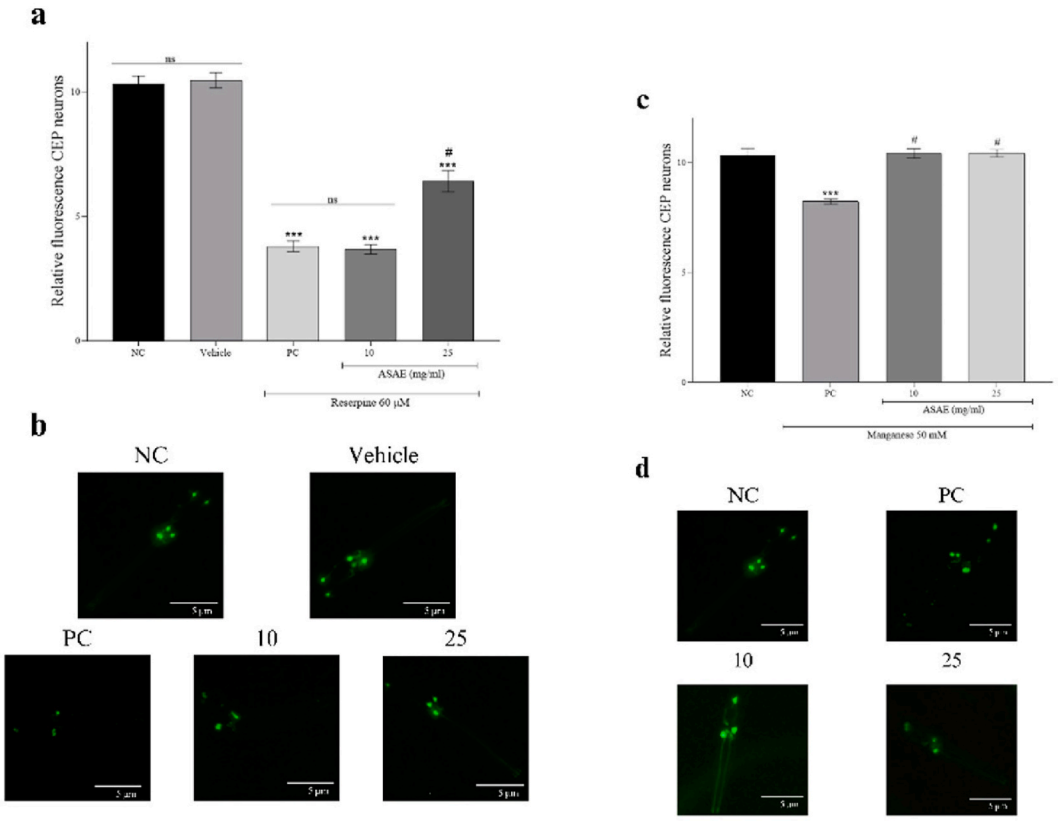

Fig. 2. Analysis and representation of dopaminergic neurodegeneration in posterior cephalic sensilla neurons (CEP) caused by RES (a, b) or manganese (c, d) with evaluation of pre-treatment with ASAE. N = 20 worms. *p < 0.05, **p < 0.01, and ***p < 0.001 *versus* the Negative Control (NC) group. #p < 0.001 *versus* the Positive Control (PC) group. ns = not significant. Values represent means ± SEM. Analyzed by one-way ANOVA followed by Dunnett's test. Scale: 1mm/5 µm.

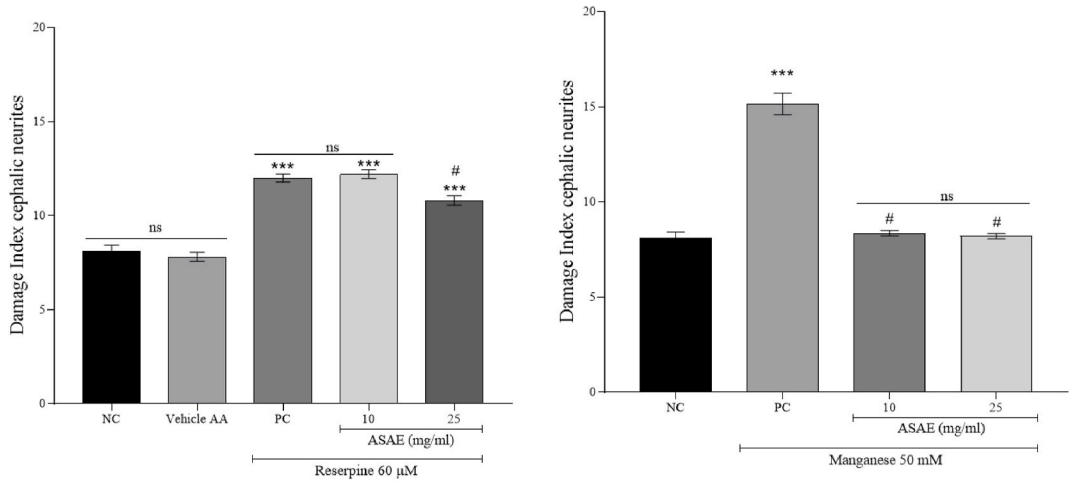

Fig. 3. Analysis of the damage index in neurites cephalic neurons caused by RES (a) or manganese (b) with evaluation of pre-treatment with ASAE. N = 20 worms. *p < 0.05, **p < 0.01, and ***p < 0.001 *versus* the Negative Control (NC) group. #p < 0.001 *versus* the Positive Control (PC) group. ns = not significant. Values represent means ± SEM. Analyzed by one-way ANOVA followed by Dunnett's test.

enzymes catalyse the hydrolysis of ketone groups within substrates. Consequently, the three main metabolites derived from ACB across various prediction algorithms are M1 (structure unknown in PubChem, https://pubchem.ncbi.nlm.nih.gov/), M2 (p-coumaric acid), and M3 (structure unknown in PubChem) (Fig. 8).

For comparative purposes, we have used drugs that are clinical references for the treatment of PD (L-dopa and apomorphine) or AD (galantamine and donepezil). Only ACB violates one (SwissADME: MW > 500) or two (Molinspiration: miLogP >5 and MW > 500) of Lipinski's Rule of Five (Table S1). Such violations would disqualify the molecule as a potential drug for crossing biological barriers through simple diffusion. In bioinformatics, different software can yield varying results for the same structure due to differences in the underlying algorithms, which may account for the observed discrepancies. Nonetheless, it is noteworthy that both online predictive tools provided similar results for the various parameters evaluated.

For miLogP, the negative value of L-dopa stands out when compared to the positive values of the other compounds. ACB exceeds the 500

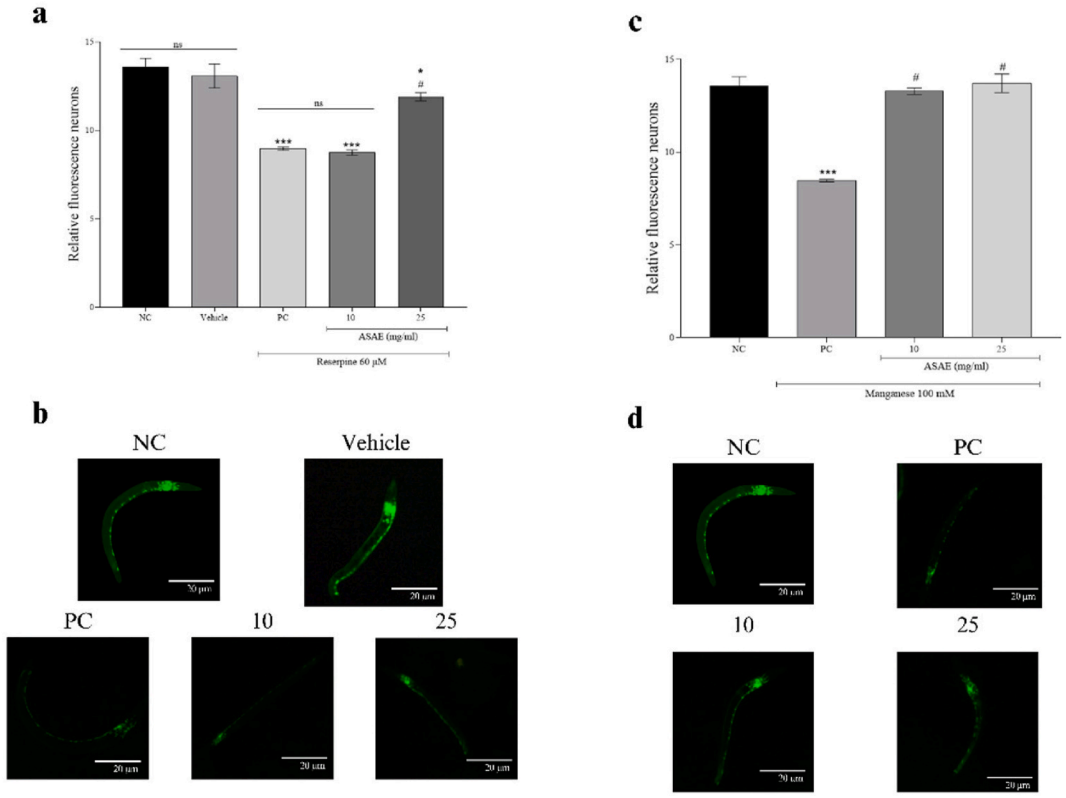

Fig. 4. Analysis and representation of cholinergic neurodegeneration in the entire animal caused by RES (a, b) or manganese (c, d) with evaluation of pre-treatment with ASAE. N = 20 worms. *p < 0.05, **p < 0.01, and ***p < 0.001 *versus* the Negative Control (NC) group. #p < 0.001 *versus* the Positive Control (PC) group. ns = not significant. Values represent means ± SEM. Analyzed by one-way ANOVA followed by Dunnett's test. Scale: 1mm/20 µm.

thresholds for molecular weight and has the highest nON value, both of which negatively impact its ability to diffuse through biological membranes. Additionally, Q and L-dopa exhibit values of 5 for nOHNH, which may further hinder their diffusion capacity (Table S1).

3.3.2. *Gastrointestinal absorption and pharmacokinetic predictions*

An important therapeutic factor is a drug's gastrointestinal absorption capacity. This complex process involves multiple variables, but it is possible to predict the permeability of the gastrointestinal tract (GIT) based on the solubility of a drug and its physicochemical characteristics. The Topological Polar Surface Area (TPSA) values of molecules are derived from the number of atoms that can engage in polar interactions. Ideal TPSA values for gastrointestinal absorption of substances that act on the CNS should range between 60 and 140 $Å^2$. All compounds of *A. satureioides* exhibit higher TPSA values than reference drugs used clinically for the treatment of AD and PD, indicating a potentially lower absorption rate (Table S2). Notably, ACB has the highest TPSA value.

Additionally, L-dopa shows higher TPSA values compared to other reference drugs. However, it is known that L-dopa employs an active transport mechanism across biological membranes via the neutral L-amino acid transporter or Large Amino Acid Transporter (LAT-1). Literature also supports the existence of transport systems for Q and L, facilitating their passage across biological barriers.

Another important indicator of gastrointestinal absorption is the number of rotations the molecule can undergo (Nrotb, Table S2). This value reflects the potential for oral bioavailability; lower values correlate with better predictions for adequate absorption. Again, ACB exhibits the highest Nrotb value among all components of the extract. Interestingly, donepezil displays a notably high number of potential rotations compared to other reference drugs, yet this does not diminish its recognized efficacy as a CNS drug.

The most water-soluble drugs are better absorbed in the gastrointestinal tract (GIT). Negative solubility values indicate poor water solubility and can predict difficulties in the absorption process. As shown in Table S3, values calculated using pkCSM software reveal that, among the reference drugs, donepezil and apomorphine exhibit the most negative solubility values. For the compounds studied here, ACB again stands out due to its high negative value.

Another indicator of absorption is the prediction of interaction with Caco-2 cells (heterogeneous human epithelial colorectal adenocarcinoma cells), where positive values indicate potential permeability through the tissues of the digestive system. Once again, ACB displays the most negative value (Table S3).

In the boiled-egg prediction shown in Fig. 9, generated using the online SwissADME software, ACB is positioned outside the egg space, while the other three components of the extract (L, Q, and 3OMQ) are located in the egg white zone (human intestinal absorption, HIA) and are very close to each other. In contrast, L-dopa, although also found in the egg white zone, is positioned much farther from the components of the extract. The other three reference drugs are situated in the egg yolk zone, indicating their ability to access the CNS through simple diffusion across the BBB. Compounds encircled in red (PGP–) are predicted not to be substrates of P-glycoprotein (P-gp), implying they are not actively expelled from the central nervous system (CNS) and may therefore remain longer in the brain. In contrast, compounds encircled in blue (PGP+) are predicted to be substrates of P-gp, making them more likely to be actively transported out of the CNS and reducing their residence time in the brain.

The percentage of drug bound to plasma proteins is a crucial indicator of drug distribution. A higher concentration of unbound drug in the bloodstream increases the likelihood of permeation through membranes and reaching target sites. As shown in Table S3, ACB and Q exhibit a higher concentration of free drug compared to the other two components of *A. satureioides*. Notably, L-dopa demonstrates the highest

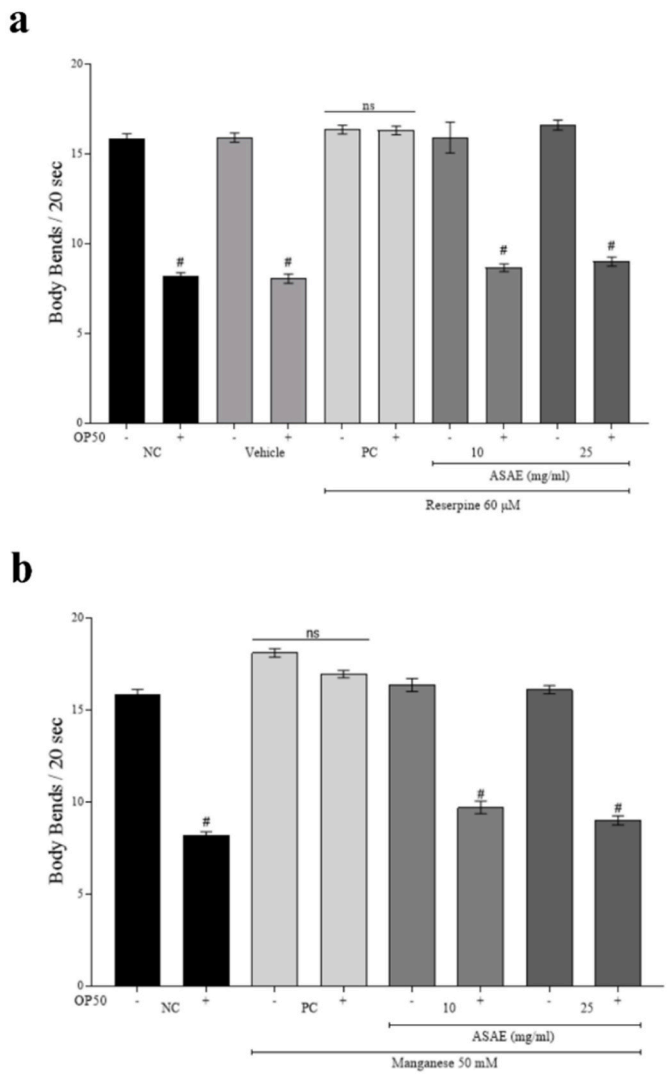

Fig. 5. Analysis of the number of body bends after damage by RES (a) or manganese (b) in the presence (+) or absence (−) of OP50, with evaluation of pre-treatment with ASAE. N = 20 worms. *p < 0.05, **p < 0.01, and ***p < 0.001 *versus* the Negative Control (NC) group. #p < 0.001 *versus* the Positive Control (PC) group with OP50. ns = not significant. Values represent means ± SEM. Analyzed by one-way ANOVA followed by Dunnett's test.

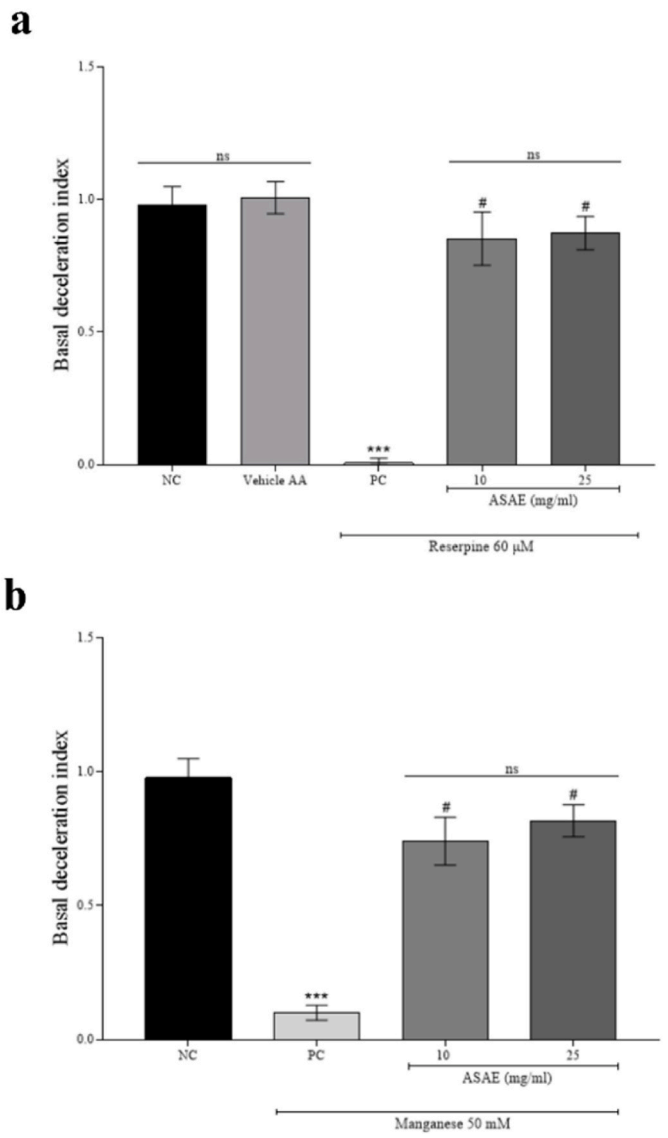

Fig. 6. Analysis of the basal deceleration index after damage by RES (a) or manganese (b) with evaluation of pre-treatment with ASAE. N = 20 worms. *p < 0.05, **p < 0.01, and ***p < 0.001 *versus* the Negative Control (NC) group. #p < 0.001 *versus* the Positive Control (PC) group with OP50. ns = not significant. Values represent means ± SEM. Analyzed by one-way ANOVA followed by Dunnett's test.

percentage of unbound drug among all evaluated molecules.

The volume of distribution (Table S3) refers to the estimated dose of a substance (in log l/kg) distributed to tissues and plasma. A higher estimate indicates greater tissue distribution. Among the compounds, ACB has the lowest value (−1.63), while Q exhibits the best value (1.55), surpassing all other tested molecules, including reference drugs.

Drug elimination is another critical factor. Substances with lower elimination rates may have prolonged effects but are also more prone to toxicity. The total clearance (C_tot) values for the evaluated molecules indicate that the flavonoids (Q, L, and 3OMQ) exhibit similar elimination profiles to L-dopa. In contrast, ACB has the lowest clearance value among all *A. satureioides* compounds and reference drugs, recorded at 0.20 log ml/min/kg.

Despite its lower absorption and distribution compared to the other molecules, ACB's pharmacological potential remains significant. With a molecular weight of 554.54, ACB is the largest molecule among those evaluated. Its structure features a linkage between two identical and symmetrical units (Fig. 8), leading us to hypothesize potential cleavage at this and other sites, resulting in various metabolites. The Biotransformer 3.0 (All Human) software predicts that ACB may engage in up to 128 interactions within human systems, 48 of which occur within the human gut microbiota (GUT) biosystem. In this context, the predominant reaction observed is keto hydrolysis, facilitated by unspecified intestinal bacterial enzymes. The nine predicted metabolites (M1 to M9, see Fig. S1) originating in the GUT can passively traverse the gastrointestinal tract (Fig. 10), as evidenced by their position in the white area of the boiled egg representation (HIA legend).

3.3.3. *Blood-brain barrier penetration and CNS targeting*

An essential factor for compounds to exert their effects in the CNS is their ability to cross the BBB. While passive diffusion is the most common and anticipated mechanism for drugs with central activity, as shown in Table 2, L-dopa only demonstrated a positive value in 1 of the 8 algorithms evaluated. Nevertheless, L-dopa is a standard reference treatment for PD, indicating its effective penetration into the CNS. In contrast, all other reference drugs yielded positive values across all evaluated algorithms.

Similarly, the compounds derived from *A. satureioides* were assessed,

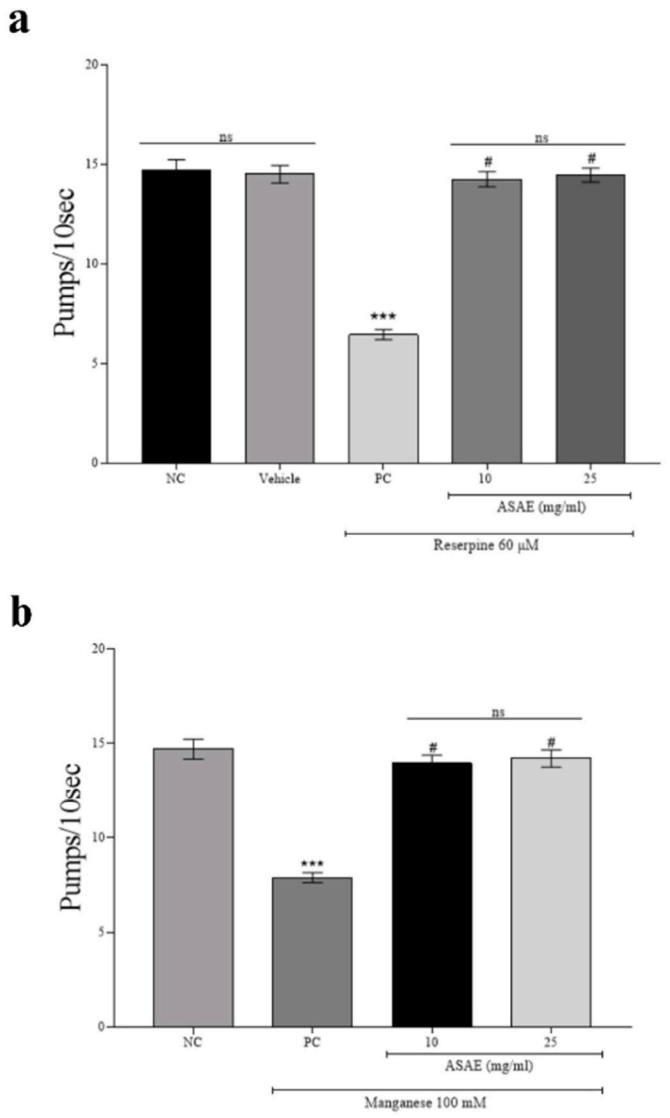

Fig. 7. Analysis of pharyngeal pumping after damage by RES (a) or manganese (b) with evaluation of pre-treatment with ASAE. N = 20 worms. *p < 0.05, **p < 0.01, and ***p < 0.001 *versus* the Negative Control (NC) group. #p < 0.001 *versus* the Positive Control (PC) group with OP50. ns = not significant. Values represent means ± SEM. Analyzed by one-way ANOVA followed by Dunnett's test.

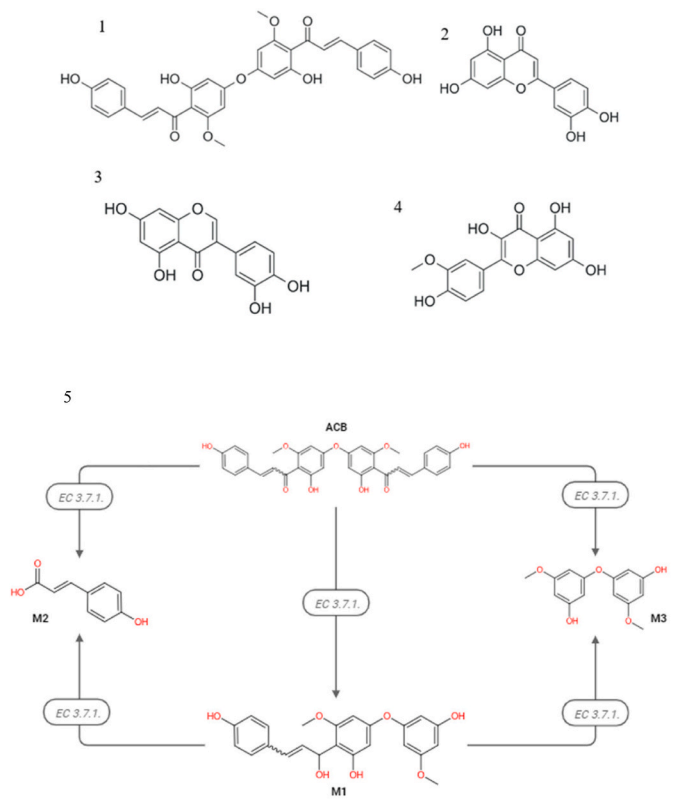

Fig. 8. Structures of bioactive compounds from ASAE obtained from ChemDraw: achyrobichalcone (ACB) (1), luteoline (L) (2), quercetin (Q) (3), 3-O-methylquercetin (3OMQ) (4), and representation of the main degradation reactions undergone by ACB within metabolization in the human biosystem, prediction with Biotransformer 3.0 (5). Note: the structure of achyrobichalcone was not in the library and was designed manually based on the structure of the first publication - Holzschuh et al. (2010).

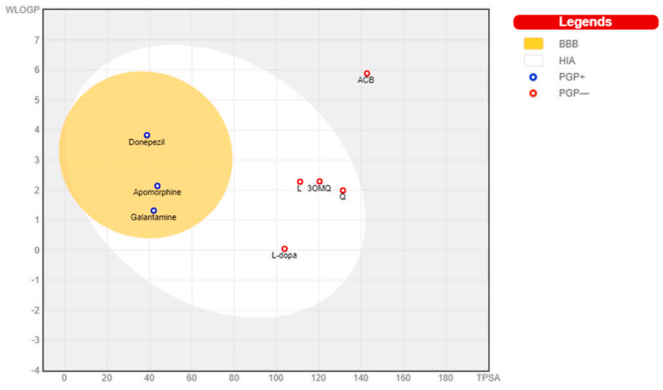

Fig. 9. Illustration of the boiled egg. Obtained from the SwissADME software, it represents the intestinal absorption capacity (egg white) and the probability of crossing the blood-brain barrier (egg yolk), by simple diffusion through the membranes. Compounds encircled in red (PGP–) are predicted not to be substrates of P-glycoprotein (P-gp). Compounds encircled in blue (PGP+) are predicted to be substrates of P-gp. (For interpretation of the references to color in this figure legend, the reader is referred to the Web version of this article.)

with ACB, and L exhibiting 5 positive values each. This performance surpassed that of 3OMQ with 2 positive values, and Q with 4 positive values.

ACB is a relatively large molecule, and although it exhibits more favourable values than L-dopa and Q regarding its ability to cross the BBB, its high molecular weight, elevated miLogP value, and negative assessment in the boiled-egg study may significantly hinder its passive diffusion. Consequently, we aimed to investigate its capacity to traverse the BBB via active transport mechanisms.

The large neutral amino acid transporter 1 (LAT1) is a membrane transporter found in various cell types, specifically designed to preferentially transport large, branched, and aromatic neutral amino acids. This transporter plays a crucial role in delivering these amino acids to proliferating cells and facilitating their passage through biological barriers, including the placenta and the BBB. LAT1 has emerged as a promising target for drugs aiming to penetrate the BBB, particularly because it remains functionally intact in several pathological conditions, such as AD. Studies have shown that L-dopa utilizes this transporter to enter the CNS, along with other prodrugs.

To assess the interactions between the compounds, present in the ASAE and LAT1, we conducted molecular docking studies, calculating the Vina scores presented in Table S4. The results indicate that the compounds from the extract demonstrate stronger interactions with the LAT1 transporter than L-dopa itself. Notably, ACB stands out with an

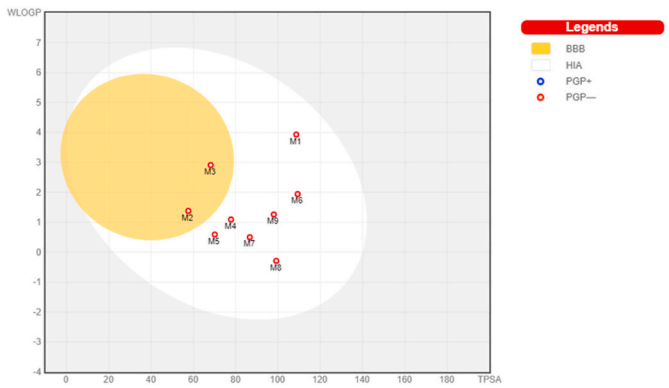

Fig. 10. Illustration of the boiled egg, obtained from the SwissADME, of primary metabolites generated exclusively within the human biosystem in Biotransformer 3.0. Compounds encircled in red (PGP–) are predicted not to be substrates of P-glycoprotein (P-gp). Compounds encircled in blue (PGP+) are predicted to be substrates of P-gp. (For interpretation of the references to color in this figure legend, the reader is referred to the Web version of this article.)

interaction score of −9.1 kcal/mol, compared to −7.0 kcal/mol for the reference ligand molecule T4. A more negative score indicates a stronger interaction, suggesting a favourable potential for ACB's transport across the BBB.

Even after successfully crossing the BBB, drugs must remain within the CNS to exert their pharmacological effects. This characteristic is critical when evaluating new therapeutic agents. Efflux pumps, such as P-glycoprotein (P-gp), are transport proteins that actively remove various physiological compounds and drugs from the brain, thereby limiting their duration of action and effectiveness within the CNS. The activity of these efflux pumps is part of the BBB's defense mechanism, which helps maintain homeostasis in the CNS.

Drugs that are susceptible to P-gp-mediated transport are typically cleared more rapidly from the CNS. Notably, none of the compounds studied here are substrates for P-glycoprotein. Furthermore, only ACB and donepezil were identified as P-glycoprotein inhibitors (Table S5), suggesting that these compounds may influence the elimination processes occurring within the CNS.

3.3.4. *Toxicological risk assessment*

Toxicity evaluation is a crucial step in the assessment of all potential new drugs. Using molecular structure data, various parameters can be predicted *in silico* to indicate the potential toxicity of these compounds. The toxicological parameters were obtained with ProTox-II.

Among the studied compounds, Q stands out negatively due to its significantly lower LD50 value compared to the others (Table S6). Notably, the reference drugs apomorphine and galantamine exhibit even lower LD50 values than Q. In contrast, ACB, L, and 3OMQ possess the highest LD50 values and classification scores, indicating that a higher-class value corresponds to reduced toxicity.

While Q, L, and 3OMQ and donepezil display potential carcinogenic activity, ACB and the three reference drugs do not exhibit any carcinogenic potential. Additionally, mutagenicity was assessed using the Ames test algorithm based on structural data, revealing that ACB, 3OMQ, donepezil, and galantamine show no mutagenic potential.

The estimated maximum recommended tolerated dose (MRTD) in humans was evaluated, revealing that none of the compounds studied displayed negative values. In contrast, the reference drugs galantamine and donepezil did show negative values (Table S6). Among all evaluated compounds, 3OMQ and L-dopa exhibited the highest tolerated doses.

The ability to inhibit the two subtypes of potassium channels (hERG I and hERG II) provides crucial information regarding the cardiotoxic potential of the compounds. ACB, 3OMQ, apomorphine, galantamine, and donepezil demonstrated the capacity to inhibit hERG II (Table S6), indicating a potential for cardiac alterations.

The liver is the primary target organ for drug toxicity, as it plays a vital role in the metabolism of many pharmaceuticals. Hepatotoxic potential was observed in three of the four reference drugs: L-dopa, galantamine, and donepezil (Table S6). Conversely, none of the compounds derived from *A. satureioides* exhibited the potential to induce liver damage.

3.3.5. *Target prediction and molecular docking analyses*

The SWISS predictor identified potential targets and mechanisms of action for ACB, 3OMQ, Q and L, with the most significant targets illustrated in Fig. 11. A total of 138 targets were predicted among the four molecules; however, only 36 showed a higher probability of selectivity and interaction according to the software algorithm. These targets were categorized based on their interaction with specific molecules. ACB displayed the greatest number of selective targets (15) compared to L (7). Notably, neither Q nor 3OMQ presented any exclusive targets. Among the targets with the highest probability, all were shared with at least one of the other molecules. In total, 10 targets were common among the four molecules, while 4 targets were shared exclusively between Q, L, and 3OMQ.

From the identified targets, the six most likely to interact with the evaluated compounds and relevant to the treatment of PD or AD were selected for molecular docking studies. These targets include dopamine receptor D_4 (DRD4), adenosine receptors A_1 and A_{2A} (ARA1/ARA2), monoamine oxidase B (MAO-B), alpha-synuclein (SNCA), and acetylcholinesterase (AChE) (Table S7). The results of the docking studies, expressed in terms of binding energy, are detailed in Table 3. Major interactions observed are illustrated in Fig. 12 and compared with previously described compounds that have demonstrated strong evidence of interaction with each target.

The binding energies associated with the selective ligands are high for the docking values, and these ligands have been previously documented in the literature as either inhibitors or activators of the receptors and enzymes analyzed here. However, it is important to note that docking studies do not predict the actual activity of the molecules (whether they act as agonists or antagonists); rather, they assess the ability of the molecules to bind to specific proteins.

Q exhibited an interaction with dopamine receptor subtype D4, achieving a binding energy of −9.3 kcal/mol, which is greater than that

Table 2
Predicted BBB-permeability parameters.

	ADABUST				SVM			
	MACCS	Openbabel	MolPrint	PubChem	MACCS	OpenBabel	MolPrint	PubChem
Quercetin	−0.997	−10.071	−0.147	−1.582	**0.003**	**0.022**	**0.086**	**0.005**
Luteolin	−0.997	−5.815	−0.147	**0.953**	**0.003**	**0.029**	**0.157**	**0.038**
3-O-methylquercetin	−2.638	−6.107	−1.803	−6.094	−0.05	**0.063**	**0.04**	−0.029
Achyrobichalcone	**0.539**	**4.839**	−0.612	−10.628	**0.002**	**0.022**	**0.346**	−0.218
L-dopa	−2.057	−1.150	−173.760	−1.221	−0.032	−0.084	**0.681**	−0.112
Apomorphine	**2.326**	**4.772**	**1.996**	**7.093**	**0.071**	**0.063**	**0.288**	**0.222**
Galantamine	**7.509**	**7.849**	**11.736**	**14.128**	**0.154**	**0.091**	**0.649**	**0.346**
Donepezil	**5.214**	**6.608**	**10.430**	**19.401**	**0.135**	**0.086**	**0.433**	**0.380**

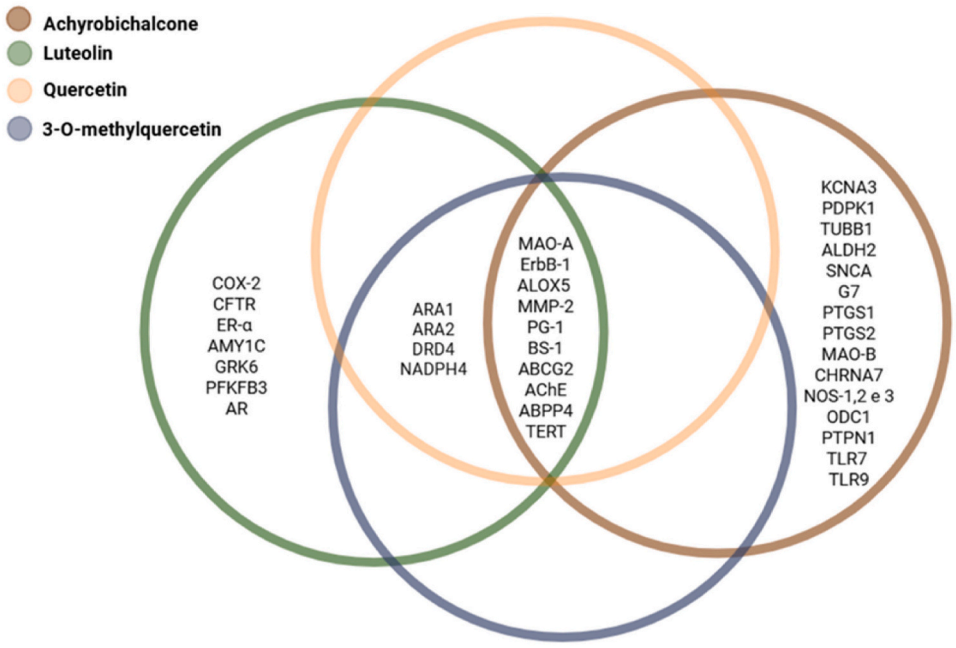

Fig. 11. Representation of achyrobichalcone (ACB), 3-O-methylquercetin (3OMQ), quercetin (Q) and luteolin (L) targets determined by SwissTargetPrediction (https://www.expasy.org/resources/swisstargetprediction).

Table 3
Binding free energy (kcal/mol) of ACB, 3OMQ, Q, L and selective ligand with the targets of interest

Target	Q	L	3OMQ	ACB	Control	
DRD4	−9.3	−9.0	−8.8	−10.3	ABT-724	−9.1
ARA1	−8.4	−8.4	−8.6	−9.1	CPA	−7.4
ARA2A	−9.5	−9.6	−9.3	−9.8	CGS 21680	−9.0
MAO-B	−9.0	−8.9	−8.2	−9.3	ISI - selegiline	−7.7
SNCA	−6.3	−6.2	−6.3	−6.7	NPT200-11	−6.3
AChE	−10.1	−10.5	−10.0	−10.9	donepezil	−10

of the control drug ABT-724 (−9.1 kcal/mol), a synthetic dopamine agonist selective for these receptors. It has previously been documented to interact with other dopamine receptors (D_1, D_2, and D_3) through molecular docking studies. Luteolin and 3OMQ demonstrated lower binding energies of −9.0 and −8.8 kcal/mol, respectively, for this receptor. Notably, ACB displayed to a binding potential that surpassed ABT-724, with a remarkable binding energy of −10.3 kcal/mol (Table 3).

The L interactions with adenosine receptors A_1 and A_{2A} yielded Vina scores that exceeded those of their selective ligands. For A_1 receptors, L, Q, and 3OMQ exhibited similar binding energies of −8.4, −8.4, and −8.6 kcal/mol, respectively, while L demonstrated a superior score for A_{2A} receptors compared to the other two. Conversely, ACB outperformed all evaluated compounds at both A_1 and A_{2A} receptors, achieving scores of −9.1 and −9.8 kcal/mol, respectively.

Regarding MAO-B interactions, 3OMQ displayed a binding energy of −8.2 kcal/mol, which is higher than that of the selective MAO-B inhibitor ISI (selegiline, −7.7 kcal/mol). A previous *in vitro* study indicated that a structurally similar flavonoid, genistein, showed selective inhibitory potential for MAO-B (IC50 = 0.65 ± 0.11) (Larit et al., 2018). All other *A. satureioides* compounds exhibited greater interaction potential, with ACB at −9.3 kcal/mol, followed by Q at −9.0 kcal/mol and L at −8.9 kcal/mol.

For the interaction with alpha-synuclein (SNCA), the control compound NPT200-11 displayed a binding energy of −6.3 kcal/mol. Flavonoids Q, L, and 3OMQ had identical binding energies to the control, while ACB demonstrated a higher potential with a binding energy of −6.7 kcal/mol.

When assessing the interaction with AChE, ACB and luteolin achieved the highest binding energies of −10.9 and −10.5 kcal/mol, respectively, surpassing the classic AChE inhibitor donepezil (−10.0 kcal/mol). In contrast, Q and 3OMQ exhibited binding energies nearly identical to that of the control.

In summary, these studies highlight ACB as the most prominent compound, exhibiting higher binding values than all evaluated controls.

4. Discussion

A. satureioides, commonly known as “Marcela”, has been traditionally utilized in Brazilian folk medicine for various health-related purposes. Studies indicate that *A. satureioides* exhibits a range of pharmacological properties, including antioxidant, anti-inflammatory, and cytoprotective effects (Zorzi et al., 2015; Arredondo et al., 2004; Bianchi et al., 2018). The plant contains flavonoids such as Q and L, which contribute significantly to its therapeutic benefits (Carini et al., 2014; Balestrin et al., 2016). Additionally, *A. satureioides* has demonstrated protective effects against UV-induced skin damage (Kadarian et al., 2002), hepatoprotective activity (Pedra et al., 2018), and selective antiglioma effects via endophytic fungi.

Exposure to RES in *C. elegans* results in significant dopamine depletion due to vesicular monoamine transporter (VMAT) blockade, causing dopaminergic damage (Reckziegel et al., 2015). Manganese has also been extensively studied for its CNS effects, with numerous assessments in *C. elegans* confirming its neurotoxic mechanism across various neurotransmitter systems. manganese exhibits a selective concentration-dependent relationship with dopaminergic neurons at 50 mM, while higher concentrations (100 mM) also damage cholinergic neurons (Benedetto et al., 2009; Schetinger et al., 2019). The Pre-treatments to ASAE partially prevented RES-induced dopaminergic and cholinergic neurodegeneration at a concentration of 25 mg/ml. Furthermore, ASAE demonstrated protective effects against neurodegeneration induced by manganese at both tested concentrations.

While the precise compounds responsible for these protective effects remain unclear due to the complexity of the multi-component extract, the modulating capacity of flavonoids on the dopaminergic system in

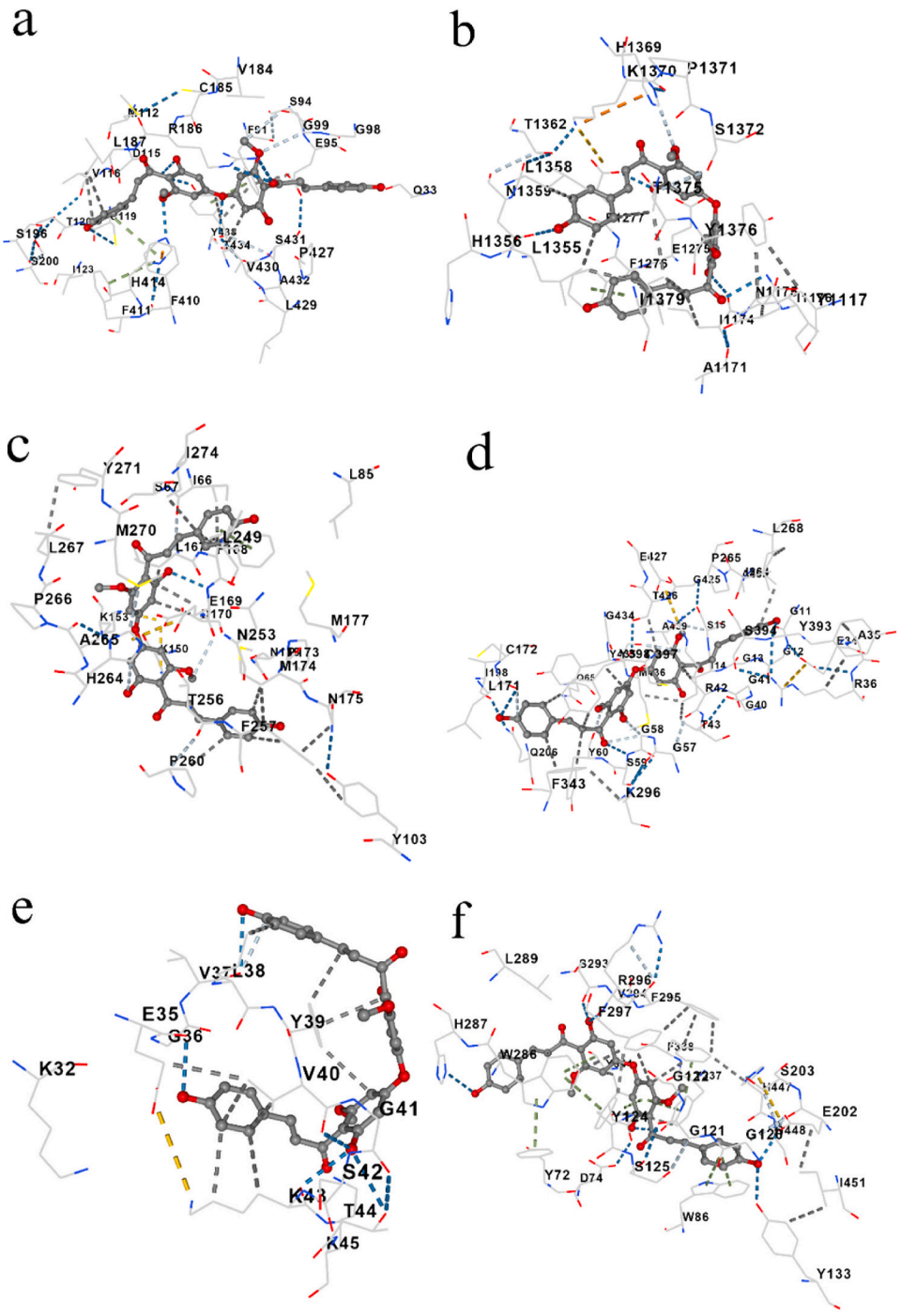

Fig. 12. Dockings representations determined by CB-Dock2 (https://cadd.labshare.cn/cb-dock2/index.php) of achyrobichalcone. The interaction is observed with dopamine D_4 receptor (a), A_1 adenosine receptor (b), A_{2A} adenosine receptor (c), monoamine oxidase B (d), α -synuclein (e) and acetylcholinesterase (f).

C. elegans has recently been highlighted (Salgueiro et al., 2023). The dopamine depletion caused by RES and manganese impairs the animals' ability to halt feeding, a behavior mediated by dopamine. ASAE treatment was able to reverse this impairment at both tested concentrations, including the 10 mg/ml treatment in the RES damage model. These results strongly suggest that ASAE may modulate dopaminergic pathways or enhance dopamine bioavailability.

Cognitive decline in PD and AD is a significant concern, as the dementias associated with PD severely impact the quality of life despite improvements in motor deficits. Disease progression and the side effects of pharmacological treatments lead to decreased acetylcholine synthesis. This depletion is linked to memory decline in animal models, further emphasizing the role of acetylcholine in cognitive function. Deficiencies in acetylcholine within the septo-hippocampal pathway and the nucleus basalis of Meynert have been associated with AD. Consequently, interventions targeting the cholinergic system, such as AChE inhibitors, aim to mitigate acetylcholine depletion and enhance cognitive processes.

Recent research has underscored the potential of *A. satureioides* for neural health. One study found that an infusion of *A. satureioides* had a protective effect on human neural cells exposed to rotenone *in vitro* (Da Cruz et al., 2024). Its neuroactive capacity has been established in models of permanent focal ischemia in rats, where the infusion reduced lesion size (as assessed by tetrazolium chloride), decreased the number

of degenerating neurons (as indicated by Fluoro-Jade staining), increased the survival of neurons, and improved motor behaviour (Rivera-Oliver and Díaz-Ríos, 2014). These findings suggest that *A. satureioides* could offer neuroprotective benefits relevant to neurodegenerative diseases or neural injuries. In addition to this, the safety of the clinical use of the extract and the effects on viral infections were recently reported, with a significant reduction in the average number of days with neurological symptoms (Bastos et al., 2023) and nociception (Bastos et al., 2025) in humans.

In *C. elegans*, pharyngeal pumping is predominantly regulated by acetylcholine. This complex feeding behavior, mediated by motor control pathways, can still occur at a cholinergic level even with dopaminergic impairment (Hills et al., 2004; Ashrafi, 2006). In the present study, ASAE treatment restored pharyngeal pumping patterns in animals damaged by RES or manganese, indicating that the extract can help reestablish the homeostasis of acetylcholine and other neurotransmitters involved in this behavior.

Two models exhibit similarities in the neurotoxic processes induced by RES and manganese, both of which alter dopamine and acetylcholine neurotransmission, resulting in oxidative stress and imbalances that contribute to neurodegeneration. It is crucial for traditional populations in Brazil—such as riverside, indigenous, and quilombola communities—to establish models for heavy metal exposure, given their recurrent environmental exposure and the lack of research on its health impacts and access to pharmacological treatments. This underscores the importance of ethnopharmacological strategies and evaluating the impact of medicinal plants on the CNS (Figueiredo et al., 2007; Bowler et al., 2015; Dorman, 2023).

The bioactive compounds in *A. satureioides*, including Q, L, 3OMQ and ACB have been evaluated *in silico* for their ADME properties and compared to drugs used in the treatment of PD and AD. While most compounds align well with drug-like properties, ACB exhibits some irregularities that could affect its candidacy as a therapeutic agent.

Regarding gastrointestinal absorption capacity, the compounds have higher Total Polar Surface Area (TPSA) values, indicating lower absorption rates compared to most reference medications. However, L-dopa shows similar TPSA values, and its active transport mechanisms across biological membranes are known (LAT-1). Compounds Q and L are also described as having active absorption processes, as they are flavonoids commonly found in human diets. In terms of drug distribution, Q showed the best Volume of Distribution (VD) value, exceeding all reference drugs. Additionally, the clearance rates of the flavonoids (Q, L and 3OMQ) were comparable to L-dopa, whereas ACB exhibited the lowest clearance value among the compounds from *A. satureioides* and reference drugs.

The toxicity assessment indicated that most compounds isolated from *A. satureioides* exhibited low toxicity levels. Q showed the highest LD50 values, while ACB, L, and 3OMQ demonstrated more favourable LD50 profiles.

ACB is a novel chalcone found exclusively in *A. satureioides*. Its pharmacological potential has been investigated for cancer therapies and is protected under patent BR 102016027068-5 A2 by a research group from the Federal University of Rio Grande do Sul. However, its effects on the CNS remain unexplored, though its potential use against glioblastomas is promising, necessitating further investigation into the basic aspects of the molecule.

ACB may have the potential to be metabolized by intestinal microbiota, leading to the production of active metabolites. Its large size and symmetrical structure suggest possible sites for degradation, potentially resulting in metabolites that can passively traverse the gastrointestinal tract. The compound's ability to cross the BBB was evaluated, with L and ACB demonstrating positive interactions with the Large Neutral Amino Acid Transporter 1 (LAT1), indicating their potential to access the CNS. Furthermore, ACB was identified as a P-glycoprotein inhibitor.

Bichalcones have been shown to inhibit enzymes such as cyclooxygenase (COX) and lipoxygenase (LOX), which are involved in the production of inflammatory mediators. They also modulate inflammatory signalling pathways, including NF-κB, leading to reduced expression of pro-inflammatory genes (Ketha et al., 2020). Q has been extensively studied for its antioxidant, anti-inflammatory, and immunomodulatory activities, contributing to its neuroprotective potential. Recent research has explored its role as a neuromodulator in the CNS (Costa et al., 2017), with strong support for its activity in neurotransmitter systems, particularly within dopaminergic pathways (Salgueiro et al., 2023).

Luteolin has been identified as a significant modulator of adenosine receptors, particularly A_1 and A_{2A} (Kim et al., 2019). These findings align with the molecular targets and docking results observed. Among the evaluated compounds, 3OMQ and ACB are associated with the general antioxidant properties of flavonoids, although their potential effects in isolation remain underexplored, especially regarding activities related to the CNS.

For the first time, the activity of ACB on these targets associated with PD and AD is reported, revealing its promise across all investigated targets (DRD4, ARA1, ARA2A, MAO-B, SNCA, and AChE), with values exceeding those of synthetic controls for each protein interaction.

One of the primary conditions underlying PD related to oxidative stress is the misfolding of alpha-synuclein (SNCA), leading to its accumulation in dopaminergic neurons and characterizing synucleinopathies. Price et al. (2018) describes the activities of an SNCA folding inhibitor (NPT200-11) that alleviates various symptoms in PD models. ACB is a recently described molecule, and its biological activities are not yet fully understood. Its neuroprotective potential has only been demonstrated once, in cultures of astrocytes and neurons, where protection was observed under oxidative.

5. Conclusion

The constituents and the *A. satureioides* aqueous extract show promising potential in neuroprotection, with flavones exhibiting concentration-dependent antioxidant activity. High concentrations produce classical antioxidant effects, while lower levels can modulate biological systems, highlighting the complexity of their regulatory roles. ACB stands out for its versatility, warranting deeper investigation into its impact on the CNS. Testing individual compounds is crucial for understanding their therapeutic and toxic profiles before they can be considered for treating PD, AD, or other neurological disorders. Comprehensive research is needed to harness their potential safely.

C.*elegans* has proven to be an effective model for studying pathways related to PD and AD. This organism allows researchers to induce dopamine and acetylcholine depletion, visualize neuronal degeneration, and assess locomotor and cognitive behaviour, making it a valuable tool for neurodegenerative research.

CRediT authorship contribution statement

Peterson Alves Santos: Writing – review & editing, Writing – original draft, Validation, Methodology, Investigation, Data curation, Conceptualization. **Pricila Pflüger:** Validation, Methodology, Investigation. **Marilise Brittes Rott:** Validation, Methodology, Conceptualization. **Hipólito Gómez-Couso:** Resources. **Ionara Rodrigues:** Resources, Project administration, Methodology, Funding acquisition. **Patricia Pereira:** Writing – review & editing, Writing – original draft, Validation, Supervision, Resources, Methodology, Formal analysis, Conceptualization. **José Ángel Fontenla:** Writing – review & editing, Writing – original draft, Validation, Supervision, Resources, Project administration, Methodology, Investigation, Funding acquisition, Formal analysis, Data curation, Conceptualization, Mariana Uczay, Validation, Methodology, Investigation.

Author agreement

All authors have read and reviewed this article and agree to its publication.

Funding information

This work was supported by Coordenação de Aperfeiçoamento de Pessoal de Nível Superior (CAPES) (number 88887.506777/2020–00); Conselho Nacional de Desenvolvimento Científico e Tecnológico (CNPq) fellowships (PhD. Patrícia Pereira; PhD. Ionara Rodrigues Siqueira; PhD. Marilise Brittes Rott) (Brazil). Resources, infrastructure and equipment from the University of Santiago de Compostela (Spain) have been used.

Declaration of competing interest

The authors declare that they have no known competing financial interests or personal relationships that could have appeared to influence the work reported in this paper.

Appendix A. Supplementary data

Supplementary data to this article can be found online at https://doi.org/10.1016/j.jep.2025.120335.

Data availability

Data will be made available on request.

References

Arredondo, M., Blasina, F., Echeverry, C., Morquio, A., Ferreira, M., Abin-Carriquiry, J. A., Laflon, L., Dajas, F., 2004. Cytoprotection by *Achyrocline satureioides* (lam.) D.C. and some of its main flavonoids against oxidative stress. J. Ethnopharmacol. 91, 13–20. https://doi.org/10.1016/j.jep.2003.11.012.

Ashrafi, K., 2006. Mapping out starvation responses. Cell Metab. 3, 235–236. https://doi.org/10.1016/j.cmet.2006.03.002.

Au, C., Benedetto, A., Anderson, J., Labrousse, A., Erikson, K., Ewbank, J., Aschner, M., 2009. SMF-1, SMF-2 and SMF-3 DMT1 orthologues regulate and are regulated differentially by manganese levels in *C. elegans*. PLoS One 4, e7792. https://doi.org/10.1371/journal.pone.0007792.

Balestrin, L., Bidone, J., Bortolin, R., Moresco, K., Moreira, J., Teixeira, H., 2016. Protective effect of a hydrogel containing *Achyrocline satureioides* extract-loaded nanoemulsion against UV-induced skin damage. J. Photochem. Photobiol. B Biol. 163, 269–276. https://doi.org/10.1016/j.jphotobiol.2016.08.039.

Bastos, C.I.M., Dani, C., Cechinel, L.R., Neves, A.H.S., Rasia, F.B., Bianchi, S.E., Loss, E.S., Lamers, M.L., Meirelles, G., Bassani, V.L., 2023. *Achyrocline satureioides* as an adjuvant therapy for the management of mild viral respiratory infections in the context of COVID-19: preliminary results of a randomized, placebo-controlled, and open-label clinical trial. Phytother Res. 37, 5354–5365. https://doi.org/10.1002/ptr.7976.

Bastos, C.I.M., Dani, C., Cechinel, L.R., Neves, A.H.S., Rasia, F.B., Lamers, M.L., Bianchi, S.E., Meirelles, G., Worm, P.V., Bassani, V.L., 2025. Validation of a traditional medicine, *Achyrocline satureioides* infusion, for the improvement of mild respiratory infection symptoms: a randomized, placebo-controlled, and open-label clinical trial. Pharmaceuticals 18 (6), 861. https://doi.org/10.3390/ph18060861.

Barioni, E.D., Santin, J.R., Machado, I.D., Rodrigues, S.F., Ferraz-de-Paula, V., Wagner, T.M., Cogliati, B., Corrêa Dos Santos, M., Machado, M.da S., de Andrade, S. F., Niero, R., Farsky, S.H., 2013. *Achyrocline satureioides* (lam.) D.C. hydroalcoholic extract inhibits neutrophil functions related to innate host defense. Evid. Based Complement. Alternat. Med. 2013, 787916. https://doi.org/10.1155/2013/787916.

Benedetto, A., Au, C., Aschner, M., 2009. Manganese-induced dopaminergic neurodegeneration: insights into mechanisms and genetics shared with parkinson's disease. Chem. Rev. 109 (10), 4862–4884. https://doi.org/10.1021/cr800536y.

Bianchi, S., Kaiser, S., Pittol, V., Doneda, E., Souza, K., Bassani, V., 2018. Semi-preparative isolation and purification of phenolic compounds from *Achyrocline satureioides* (lam) D.C. by high-performance counter-current chromatography. Phytochem. Anal. 30 (2), 182–192. https://doi.org/10.1002/pca.2803.

Bowler, R., Kornblith, E., Gocheva, V., Colledge, M., Bollweg, G., Kim, Y., Lobdell, D., 2015. Environmental exposure to manganese in air: associations with cognitive functions. Neurotoxicol 49, 139–148. https://doi.org/10.1016/j.neuro.2015.06.004.

Brochard, V., Combadière, B., Prigent, A., Laouar, Y., Perrin, A., Beray-Berthat, V., Bonduelle, O., Alvarez-Fischer, D., Callebert, J., Launal, J.M., Duyckaerts, C., Flavell, R.A., Hirsch, E., Hunot, S., 2008. Infiltration of CD4+ lymphocytes into the brain contributes to neurodegeneration in a mouse model of parkinson disease. J. Clin. Investig. https://doi.org/10.1172/jci36470.

Carini, J., Klamt, F., Bassani, V., 2014. Flavonoids from *achyrocline satureioides*: promising biomolecules for anticancer therapy. RSC Adv. 4 (7), 3131–3144. https://doi.org/10.1039/c3ra43627f.

Cooper, J.F., Van Raamsdonk, J.M., 2018. Modeling parkinson's disease in *C. elegans*. J. Parkinsons Dis. 8 (1), 17–32. https://doi.org/10.3233/jpd-171258.

Costa, L., Garrick, J., Roqué, P., Pellacani, C., 2016. Mechanisms of neuroprotection by quercetin: counteracting oxidative stress and more. Oxid. Med. Cell. Longev. 2016, 1–10. https://doi.org/10.1155/2016/2986796.

Costa, S., Oliveira, I., Nascimento, L., Barros, D., Costa, R., 2017. General aspects of quercetin and its biological activities. Anais do 5° Encontro Brasileiro Para Inovação Terapêutica. ISSN, pp. 2318–3926. https://doi.org/10.17648/ebit-2017-85661.

Da Cruz, I.B.M., Chelotti, M.E., Turra, B.O., Bonotto, N.C.A., Pulcinelli, D.F., Escher, A.L. K., Klein, C., Mello, P.A., Bitencourt, G.R., Barbisan, F., 2024. *Achyrocline satureioides* infusion, popularly prepared and consumed, has an *in vitro* protective effect on human neural cells exposed to rotenone. J. Ethnopharmacol. 332, 118350. https://doi.org/10.1016/j.jep.2024.118350.

Driver, J.A., Logroscino, G., Gaziano, J.M., Kurth, T., 2009. Incidence and remaining lifetime risk of parkinson disease in advanced age. Neurology 72 (5), 432–438. https://doi.org/10.1212/01.wnl.0000341769.50075.bb.

Dorman, D.C., 2023. The role of oxidative stress in manganese neurotoxicity: a literature review focused on contributions made by professor michael aschner. Biomolecules 13 (8), 1176. https://doi.org/10.3390/biom13081176.

Figueiredo, B., Borba, R., Angélica, R., 2007. Arsenic occurrence in Brazil and human exposure. Environ. Geochem. Health 29 (2), 109–118. https://doi.org/10.1007/s10653-006-9074-9.

Gavet, O., Pines, J., 2010. Progressive activation of CyclinB1-Cdk1 coordinates entry to mitosis. Dev. Cell 18 (4), 533–543. https://doi.org/10.1016/j.devcel.2010.02.013.

Gross, A.V., Stolz, E.D., Müller, L.G., Rates, S.M.K., Ritter, M.R., 2019. Medicinal plants for the "nerves": a review of ethnobotanical studies carried out in southern Brazil. Acta Bot. Bras. 33 (2), 269–282. https://doi.org/10.1590/0102-33062018abb0386.

Guedes, E.C., Erustes, A.G., Leão, A.H.F.F., Carneiro, C.A., Abílio, V.C., Zuardi, A.W., Hallak, J.E.C., Crippa, J.A., Bincoletto, C., Smaili, S.S., 2023. Cannabidiol recovers dopaminergic neuronal damage induced by reserpine or α-synuclein in *Caenorhabditis elegans*. Neurochem. Res. 48 (8), 2390–2405. https://doi.org/10.1007/s11064-023-03905-z.

Hills, T.T., Brockie, P.J., Maricq, A.V., 2004. Dopamine and glutamate control area-restricted search behavior in *Caenorhabditis elegans*. J. Neurosci. 24 (5), 1217–1225. https://doi.org/10.1523/jneurosci.1569-03.2004.

Holzschuh, M.H., Gosmann, G., Schneider, P.H., Schapoval, E.E.S., Bassani, V.L., 2010. Identification and stability of a new bichalcone in *Achyrocline satureioides* spray dried powder. Pharmazie 65 (9), 650–656. https://doi.org/10.1691/ph.2010.0085.

Kadarian, C., Broussalis, A., Miño, J., López, P., Gorzalczany, S., Ferraro, G., Acevedo, C., 2002. Hepatoprotective activity of *Achyrocline satureioides* (lam) D.C. Pharmacol. Res. 45 (1), 57–61. https://doi.org/10.1006/phrs.2001.0904.

Ketha, A., Vedula, G.S., Sastry, A.V.S., 2020. *In vitro* antioxidant, anti-inflammatory, and anticancer activities of methanolic extract and its metabolites of whole plant *Cardiospermum canescens* wall. Fut. J. Pharm. Sci. 6 (1), 1–8. https://doi.org/10.1186/s43094-020-00028-y.

Khanna, N., Cressman III, C.P., Tatara, C.P., Williams, P.L., 1997. Tolerance of the nematode *Caenorhabditis elegans* to pH, salinity, and hardness in aquatic media. Arch. Environ. Contam. Toxicol. 32 (1), 110–114. https://doi.org/10.1007/s002449900162.

Kim, T.H., Custodio, R.J., Cheong, J.H., Kim, H.J., Jung, Y.S., 2019. Sleep promoting effect of luteolin in mice via adenosine A_1 and A_{2A} receptors. Biomol. Ther. (Seoul) 27 (6), 584–590. https://doi.org/10.4062/biomolther.2019.149.

Kim, T., Leem, E., Lee, J., Kim, S., 2020. Control of reactive oxygen species for the prevention of Parkinson's disease: the possible application of flavonoids. Antioxidants 9 (7), 583. https://doi.org/10.3390/antiox9070583.

Krawczuk, D., Groblewska, M., Mroczko, J., Winkel, I., Mroczko, B., 2024. The role of α-synuclein in etiology of neurodegenerative diseases. Int. J. Mol. Sci. 25 (17), 9197. https://doi.org/10.3390/ijms25179197.

Larit, F., Elokely, K.M., Chaurasiya, N.D., Benyahia, S., Nael, M.A., León, F., Abu-Darwish, M.S., Efferth, T., Wang, Y.H., Belouahem-Abed, D., Benayache, S., Tekwani, B.L., Cutler, S.J., 2018. Inhibition of human monoamine oxidase A and B by flavonoids isolated from two Algerian medicinal plants. Phytomedicine 40, 27–36. https://doi.org/10.1016/j.phymed.2017.12.032.

Martínez-Busi, M., Arredondo, F., González, D., Echeverry, C., Vega-Teijido, M.A., Carvalho, D., Rodríguez-Haralambides, A., Rivera, F., Dajas, F., Abin-Carriquiry, J. A., 2019. Purification, structural elucidation, antioxidant capacity and neuroprotective potential of the main polyphenolic compounds contained in *Achyrocline satureioides* (lam) D.C. (compositae). Bioorg. Med. Chem. 27 (12), 2579–2591. https://doi.org/10.1016/j.bmc.2019.03.047.

Megret, F.R., Correa, D.T., Carriquiri, J.A.A., dos Santos, G.P., Busi, M.M., Méndez, F.D., 2013. Achyrocline satureioides (lam.) DC. (marcela) reduces brain damage in permanent focal ischemia in rats. Rev. Cubana Plantas Med. 18 (3), 445–460. https://www.medigraphic.com/cgi-bin/new/resumen.cgi?IDARTICULO=45387.

Moresco, K.S., Silveira, A.K., Zeidán-Chuliá, F., Correa, A.P.F., Oliveira, R.R., Borges, A. G., Grun, L., Barbé-Tuana, F., Zmozinski, A., Brandelli, A., Vale, M.G.R., Gelain, D.P., Bassani, V.L., Moreira, J.C.F., 2017. Effects of *Achyrocline satureioides* inflorescence extracts against pathological intestinal bacteria: chemical characterization, *in vitro* test, and *in vivo* evaluation. Evid. Based Complement. Alternat. Med. 2017. https://doi.org/10.1155/2017/4874865. ID 4874865.

National Health Surveillance Agency (ANVISA), 2024. Brazilian pharmacopoeia phytotherapeutic formulary. ANVISA. Brasília, Brazil, p. 27. http://bibliotecadigital.anvisa.gov.br/jspui/handle/anvisa/12413.

Park, S., Schulz, E., Lee, D., 2007. Disruption of dopamine homeostasis underlies selective neurodegeneration mediated by α-synuclein. Eur. J. 26 (11), 3104–3112. https://doi.org/10.1111/j.1460-9568.2007.05929.x.

Pedra, N., Galdino, K., Silva, D., Ramos, P., Bona, N., Soares, M., Azambuja, J.J., Canuto, K.M., Brito, E.S., Ribeiro, P.R.V., Souza, A.S.Q., Cunico, W., Stefanello, F.M., Spanavello, R.M., Braganhol, E., 2018. Endophytic fungus isolated from *Achyrocline satureioides* exhibits selective antiglioma activity—the role of SCH-642305. Front. Oncol. 8. https://doi.org/10.3389/fonc.2018.00476.

Price, D.L., Koike, M.A., Khan, A., Wrasidlo, W., Rockenstein, E., Masliah, E., Bonhaus, D., 2018. The small molecule alpha-synuclein misfolding inhibitor, NPT200-11, produces multiple benefits in an animal model of parkinson's disease. Sci. Rep. 8 (1), 16165. https://doi.org/10.1038/s41598-018-34490-9.

Reckziegel, P., Chen, P., Caito, S., Gubert, P., Soares, F.A.A., Fachinetto, R., Aschner, M., 2015. Extracellular dopamine and alterations on dopamine transporter are related to reserpine toxicity in *Caenorhabditis elegans*. Arch. Toxicol. 90 (3), 633–645. https://doi.org/10.1007/s00204-015-1451-7.

Retta, D., Dellacassa, E., Villamil, J., Suárez, S.S., Bandoni, A.L., 2012. Marcela, a promising medicinal and aromatic plant from Latin America: a review. Ind. Crop. Prod. 38, 27–38. https://doi.org/10.1016/j.indcrop.2012.01.006.

Rivera-Oliver, M., Díaz-Ríos, M., 2014. Using caffeine and other adenosine receptor antagonists and agonists as therapeutic tools against neurodegenerative diseases: a review. Life Sci. 101 (1–2), 1–9. https://doi.org/10.1016/j.lfs.2014.01.083.

Salgueiro, W.G., Soares, M.V., Martins, C.F., Paula, F.R., Rios-Anjos, R.M., Carrazoni, T., Mori, M.A., Müller, R.U., Aschner, M., Dal Belo, C.A., Ávila, D.S., 2023. Dopaminergic modulation by quercetin: *in silico* and *in vivo* evidence using *Caenorhabditis elegans* as a model. Chem. Biol. Interact. 382, 110610. https://doi.org/10.1016/j.cbi.2023.110610.

Santos, P.A., Uczay, M., Pflüger, P., Lobo, L.A.C., Rott, M.B., Fontenla, J.A., Siqueira, I.R., Pereira, P., 2024. Toxicological assessment of the *Achyrocline satureioides* aqueous extract in the *Caenorhabditis elegans* alternative model. J. Toxicol. Environ. Health A 87 (18), 730–751. https://doi.org/10.1080/15287394.2024.2368618.

Sammi, S.R., Jameson, L.E., Conrow, K.D., Leung, M.C.K., Cannon, J.R., 2022. *Caenorhabditis elegans* neurotoxicity testing: novel applications in the adverse outcome pathway framework. Front. Toxicol. 4 (1), 8. https://doi.org/10.3389/ftox.2022.826488.

Sawin, E.R., Ranganathan, R., Horvitz, H.R., 2000. *C. elegans* locomotory rate is modulated by the environment through a dopaminergic pathway and by experience through a serotonergic pathway. Neuron 26 (3), 619–631. https://doi.org/10.1016/s0896-6273(00)81199-x.

Schetinger, M.R.C., Peres, T.V., Arantes, L.P., Carvalho, F., Dressler, V., Heidrich, G., Bowman, A.B., Aschner, M., 2019. Combined exposure to methylmercury and manganese during L1 larval stage causes motor dysfunction, cholinergic and monoaminergic up-regulation and oxidative stress in L4 *Caenorhabditis elegans*. Toxicol 411, 154–162. https://doi.org/10.1016/j.tox.2018.10.006.

Zhang, X., Chen, J., Ouyang, D., Lu, J., 2020. Quercetin in animal models of Alzheimer's disease: a systematic review of preclinical studies. Int. J. Mol. Sci. 21 (2), 493. https://doi.org/10.3390/ijms21020493.

Zorzi, G., Caregnato, F., Moreira, J., Teixeira, H., Carvalho, E., 2015. Antioxidant effect of nanoemulsions containing extract of *Achyrocline satureioides* (lam) DC—Asteraceae. AAPS PharmSciTech 17 (4), 844–850. https://doi.org/10.1208/s12249-015-0408-8.

Glossary

3OMQ: 3-O-methylquercetin
ACB: Achyrobichalcone
AChE: Acetylcholinesterase
AD: Alzheimer's Disease
ADE: Anterior Deirid Neurons
ADME: Absorption, Distribution, Metabolism, and Elimination
ANOVA: Analysis of Variance
ARA1: Adenosine Receptor A_1
ARA2A: Adenosine Receptor A_{2A}
A.satureioides: Achyrocline satureioides
ASAE: Achyrocline satureioides Aqueous Extract
BBB: Blood-Brain Barrier
C. elegans: Caenorhabditis elegans
CEP: Cephalic Sensilla Neurons
CNS: Central Nervous System
C_tot: Total Clearance
DRD4: Dopamine Receptor D_4
GFP: Green Fluorescent Protein
hERG: Human Ether-à-go-go-Related Gene (potassium channels)
HIA: Human Intestinal Absorption
L: Luteolin
LAT1: Large Neutral Amino Acid Transporter 1
LD50: Lethal Dose 50 %
MAO-B: Monoamine Oxidase B
MRTD: Maximum Recommended Tolerated Dose
MW: Molecular Weight
NGM: Nematode Growth Medium
nOHNH: Hydrogen Bond Donors
nON: Hydrogen Bond Acceptors
Nrotb: Number of Rotatable Bonds
OP50: Escherichia coli strain OP50
PD: Parkinson's Disease
PDE: Post-Deirid Neurons
P-gp: P-glycoprotein
Q: uercetin
RES: Reserpine
SEM: Standard Error of the Mean
SNCA: Alpha-synuclein
SVM: Support Vector Machine
TPSA: Topological Polar Surface Area
UHPLC: Ultra High-Performance Liquid Chromatography
VDss: Volume of Distribution at Steady State
VMAT: Vesicular Monoamine Transporter